The Astrophysical Journal, 697:1242–1255, 2009 June 1 doi:10.1088/0004-637X/697/2/1242

HIGH ABUNDANCES OF CIRCUMSTELLAR AND INTERSTELLAR C-ANOMALOUS PHASES IN THE PRIMITIVE CR3 CHONDRITES QUE 99177 AND MET 00426

Christine Floss[1], and Frank J. Stadermann
Laboratory for Space Sciences and Physics Department, Washington University, St. Louis, MO 63130, USA; floss@wustl.edu
Received 2008 November 21; accepted 2009 March 16; published 2009 May 11

ABSTRACT

QUE 99177 and MET 00426 are the first known CR3 chondrites and have largely escaped the aqueous alteration experienced by most of the CR chondrite group. In addition to high presolar silicate and oxide grain abundances, these meteorites also contain high abundances of phases with anomalous C isotopic compositions. Presolar SiC abundances (∼65 ppm) are consistent with independent estimates for CR1 and CR2 chondrites, indicating that aqueous alteration does not destroy SiC, but are significantly higher than earlier abundance estimates based on noble gas contents. Particularly notable are the high abundances (∼120 ppm) of carbonaceous matter with anomalous C isotopic compositions that probably formed in cold molecular clouds via ion–molecule reactions. The observation of both ^{13}C-enriched and ^{13}C-depleted compositions suggests that multiple chemical pathways contribute to the formation of this material. The abundance of such material is significantly higher in QUE 99177 and MET 00426 than in other primitive meteorites and attests to the primitive nature of the CR3 chondrites.

Key words: astrochemistry – circumstellar matter – ISM: general

1. INTRODUCTION

The C-rich phases SiC and graphite were among the first forms of stardust identified in primitive meteorites (Bernatowicz et al. 1987; Amari et al. 1990) and are usually present in concentrations of ⩽10–20 ppm (e.g., Zinner 2004). For the most part these grains formed in the outflows of asymptotic giant branch (AGB) stars, or in the ejecta of type II supernovae (see Lodders & Amari 2005, for a review). In addition to these circumstellar grains, there exists also a much smaller population of presolar matter with C isotopic anomalies that is thought to have an interstellar origin. This material, which to date has been identified only in interplanetary dust particles (IDPs; Floss et al. 2004) and in the insoluble organic matter (IOM) of primitive meteorites (Busemann et al. 2006b), is associated with N isotopic anomalies and is generally thought to have formed via low temperature ion–molecule reactions in cold molecular clouds. N- and H-anomalous matter without C isotopic anomalies, also of likely interstellar origin, is much more abundant and is well-known from IDPs as well as primitive meteorites (e.g., Aléon et al. 2001, 2003; Messenger et al. 2003; Floss et al. 2006; Busemann et al. 2006a).

QUE 99177 and MET 00426 are the first known CR3 chondrites (Abreu & Brearley 2008). Compared to other members of this meteorite group, which have generally experienced extensive aqueous alteration, both are largely unaltered. Abreu & Brearley (2006) noted that, unlike other CR chondrites, the matrix material of these two meteorites contains few phyllosilicates, but is instead dominated by amorphous silicates similar to those found in other primitive chondrites that contain abundant presolar grains, such as Acfer 094 and ALHA77307. Transmission electron microscopy (TEM) observations show that the carbonaceous matter in these two meteorites also seems to be quite primitive, with a low degree of crystallinity and detectable concentrations of elements such as N, O, and S that are usually lost during high temperature processing (Abreu and Brearley, 2006). High amino acid contents in these meteorites indicate that their soluble organic matter is also very primitive (Martins et al. 2008). In keeping with the primitive nature of these meteorites, we found both of them to contain very high abundances of O-rich presolar grains, similar to or even exceeding those observed in other primitive chondrites (Floss & Stadermann 2009a). Here, we report on our investigation of phases with anomalous C isotopic abundances. Our study provides the first extensive in situ characterization of C-rich circumstellar and interstellar grains. Preliminary results were presented by Floss & Stadermann (2008).

2. EXPERIMENTAL

We obtained a polished thin section of each meteorite from the Johnson Space Center Meteorite Curation Facility, section 26 from QUE 99177 and section 24 from MET 00426. Each section was initially documented with an Olympus BH2 optical microscope in order to locate candidate matrix areas for presolar grain searches.

We used the Washington University Cameca NanoSIMS 50 ion microprobe to locate isotopically anomalous grains. The measurements were carried out in raster imaging mode by scanning a ∼1 pA Cs^+ primary ion beam (∼100 nm diameter) over individual matrix areas and collecting negative secondary ions as well as secondary electrons (SE). Sample areas of 12 × 12 μm^2 were presputtered using a high beam current (∼10 pA) to remove the carbon coating on regions of interest. Analyses then consisted of multiple (usually five) scans of 10 × 10 μm^2 (256^2 pixels) areas within the presputtered region that were added together to form one image measurement. Mass peaks were automatically centered on one or two reference masses ($^{12}C^-$, $^{16}O^-$, and/or $^{12}C^{14}N^-$) after each scan and the positions of the masses on the other detectors were calibrated accordingly. The analyses were carried out in automated mapping mode, with automatic stage movement to subsequent matrix areas, following a predefined grid pattern on the sample. Grains with isotopically anomalous $^{12}C/^{13}C$ ratios were identified from both C and O ($^{12}C^-$, $^{13}C^-$, $^{16}O^-$, $^{17}O^-$, $^{18}O^-$) and C and N ($^{12}C^-$, $^{13}C^-$, $^{12}C^{14}N^-$, $^{12}C^{15}N^-$, $^{28}Si^-$) imaging routines. The total matrix area analyzed for C isotopes is 15,400 μm^2 from QUE 99177 and 12,900 μm^2 from MET 00426. Carbon isotopic

[1] Author to whom any correspondence should be addressed.

compositions are normalized to the average composition of the matrix material from each meteorite, assuming normal bulk isotopic compositions. This approach is justified since we are looking only for very anomalous presolar components that are present at ppm levels in the matrix. Nitrogen isotopic compositions are normalized to a synthetic silicon nitride (Si_3N_4) standard. Grains are considered presolar if their compositions deviate from the average surrounding material by more than 4σ and if the anomaly is present in three or more consecutive image scans.

Isotopically anomalous grains were analyzed for their elemental compositions using the PHI 700 Auger Nanoprobe at Washington University. The areas of interest were initially briefly sputter cleaned with a defocused 2kV 1μA Ar^+ ion beam to remove atmospheric surface contamination. Auger electron energy spectra from 30 to 1730 eV were obtained with a 10 kV 0.25 nA primary electron beam which was rastered over the grains of interest; because the low beam current results in a low signal-to-noise ratio, multiple scans of a given grain are added together to obtain a single Auger spectrum. These analysis protocols were initially implemented to reduce the possibility of electron beam damage on fragile presolar silicate grains, which occasionally produced artifacts in the Auger spectra under high beam currents (Stadermann et al. 2009), but have been adopted here as well, as our standard operating procedures. For the most part we do not provide quantitative elemental concentrations for the C-anomalous grains, but have merely used the Auger spectra to qualitatively identify the type of presolar grain associated with each isotopic anomaly (e.g., SiC or carbonaceous grains). In the case of carbonaceous grains, we further qualitatively identify the relative abundances of the elements (e.g., C, N, O) present in the spectra. Quantitative data are not provided for two reasons. First, we do not have sensitivity factors from standards similar in composition to most of these grains. In addition, because of the backscatter effect (Stadermann et al. 2009) and other possible sources of surface contamination (e.g., atmospheric or formation of a thin oxide layer on the grains), we are not able to accurately assess how much oxygen in the spectra is intrinsically associated with the grains. We note, for example, that SiC grains embedded in meteorite matrix material typically show the presence of ~10–15 at.% O in their Auger spectra whereas grains mounted on Au foil show lower O abundances, but are still not entirely O-free.

We also obtained high-resolution Auger elemental distribution maps (3×3 μm^2 or 5×5 μm^2; 256^2 pixels) of selected elements (e.g., O, C, N, S, Si, Fe, Mg) for many of the grains. Auger mapping was carried out at 10 kV with a 5 nA primary beam and generally consisted of between 5 and 30 scans over the area of interest, depending on the sensitivity of the element being mapped. These maps provide detailed qualitative information about the distribution of elements within and around the grains, and in some cases helped to identify very small grains that were difficult to locate with SE images alone.

3. RESULTS AND DISCUSSION

We found a total of 69 areas with anomalous C isotopic compositions, 34 from QUE 99177 and 35 from MET 00426. Information about the regions, including size, isotopic composition, and elemental make-up, is given in Table 1; in addition, their isotopic compositions are plotted in Figure 1. Grains are identified by the matrix area in which they were measured (e.g., "2", "5b," "6e"), followed by the specific raster ion image in that matrix area and, finally, by grain number (e.g., "c1," "c2").

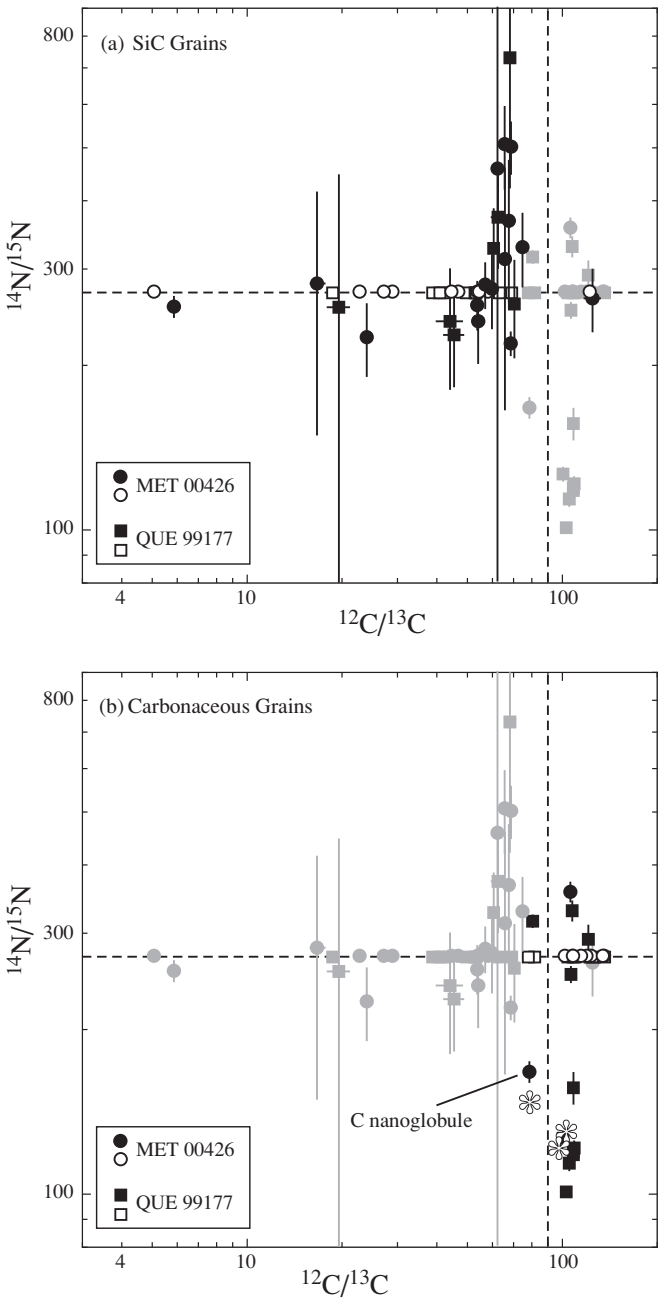

Figure 1. Plots of $^{12}C/^{13}C$ vs. $^{14}N/^{15}N$ ratios showing the distributions of (a) SiC and (b) carbonaceous grains in QUE 99177 (squares) and MET 00426 (circles). Stars show three carbonaceous grains found in IDPs (Floss et al. 2004, 2006) and in the insoluble organic matter from CR2 chondrite EET 92042 (Busemann et al. 2006b). The dashed lines indicate normal (terrestrial) values. Grains represented by the open symbols are those for which no N isotopic data are available and are arbitrarily plotted on the terrestrial N composition line. Errors are 1σ.

Nitrogen isotopes were measured in 35 of the grains (those shown as black symbols in Figure 1). About 2/3 of the grains are ^{13}C-rich, with $^{12}C/^{13}C$ ratios between 5 and 82; the remaining 1/3 are ^{12}C-rich with ratios from 101 to 136 (Table 1). Although there are exceptions, in general those grains that are enriched in ^{13}C have low N abundances (reflected in the large errors on their isotopic compositions) with mostly normal N isotopic compositions, whereas grains that are enriched in ^{12}C generally have higher N abundances and often exhibit enrichments in ^{15}N.

Table 1
C-Anomalous Grains from QUE 99177 and MET 00426

Grain	Size (nm)	$^{12}C/^{13}C$	$\delta^{13}C$[a]	$^{14}N/^{15}N$	$\delta^{15}N$[a]	Phase[b]	Elements[c]
(a) C-anomalous grains from QUE 99177							
5-7c1	150	49.6 ± 2.2	815 ± 80	n.m.	n.m.	SiC, ms	
5-13c1	350 × 200	104 ± 2	−135 ± 20	n.m.	n.m.	*Carbonaceous*	O, C
5-18c1	150	42.3 ± 2.7	1130 ± 135	n.m.	n.m.	*SiC, ms*	
5b-1c1	190	40.9 ± 2.8	1200 ± 150	n.m.	n.m.	SiC, ms	
5b-3c1	550 × 350	81.7 ± 1.0	102 ± 15	n.m.	n.m.	Carbonaceous	C, O, N
5b-10c1	270	78.0 ± 1.7	155 ± 25	n.m.	n.m.	Carbonaceous	C, O, (N)
5b-10c2	450 × 200	110 ± 4	−180 ± 30	n.m.	n.m.	*Carbonaceous*	n.m.
6-2c1	150	69.1 ± 2.9	300 ± 55	n.m.	n.m.	SiC, ms	
6-3c1	150	38.8 ± 3.1	1320 ± 180	n.m.	n.m.	*SiC, ms*	
6-5c1	200	63.1 ± 2.3	425 ± 50	n.m.	n.m.	SiC, ms	
7-1c1	400 × 350	108 ± 2	−170 ± 15	n.m.	n.m.	Carbonaceous	C, O, (N)
7-10c1	250 × 100	125 ± 4	−280 ± 25	n.m.	n.m.	Carbonaceous	C, O, (N)
7b-2c1	150 × 100	18.7 ± 0.6	3820 ± 145	n.m.	n.m.	SiC, ms	
7b-2c2	230	52.8 ± 3.2	705 ± 105	n.m.	n.m.	SiC, ms	
8-4c1	200	136 ± 10	−340 ± 50	n.m.	n.m.	Carbonaceous	C, O
8-16c1	230	53.3 ± 1.0	690 ± 30	n.m.	n.m.	SiC, ms	
5a-2c1	250	105 ± 2	−145 ± 20	114 ± 4	1380 ± 80	Carbonaceous	C, O
5a-3c1	590	107 ± 2	−155 ± 20	253 ± 9	75 ± 40	*Carbonaceous*	n.m.
5a-7c1	660	101 ± 1	−105 ± 10	127 ± 4	1145 ± 70	Carbonaceous	C, O, N
5a-10c1	280	107 ± 3	−160 ± 25	331 ± 15	−175 ± 35	*Carbonaceous*	O, C
5b-1c1	450	68.2 ± 2.4	320 ± 45	732 ± 310	−630 ± 160	SiC, ms	
5b-2c1	160	19.5 ± 1.6	3600 ± 390	256 ± 192	60 ± 800	SiC, ms	
5b-4c1	300	80.5 ± 1.1	120 ± 15	316 ± 9	−140 ± 25	Carbonaceous	C, O
5b-6c1	200 × 150	108 ± 3	−170 ± 20	157 ± 11	735 ± 120	Carbonaceous	C, O
5b-8c1	190	62.5 ± 3.2	440 ± 75	374 ± 73	−275 ± 140	SiC, ms	
5c-6c1	800	108 ± 3	−170 ± 20	118 ± 3	1300 ± 60	*Carbonaceous*	n.m.
5c-6c2	380	109 ± 3	−175 ± 20	122 ± 4	1235 ± 75	*Carbonaceous*	n.m.
5c-12c1	190	70.4 ± 3.0	280 ± 55	260 ± 53	50 ± 215	SiC, ms	
5c-18c1	190	44.0 ± 4.4	1045 ± 205	241 ± 60	125 ± 285	*SiC, ms*	
6b-3c1	270	103 ± 2	−125 ± 15	101 ± 2	1690 ± 60	*Carbonaceous*	n.m.
6b-4c1	400 × 100	108 ± 3	−170 ± 20	120 ± 4	1270 ± 80	*Carbonaceous*	n.m.
6b-9c1	160	60.6 ± 1.9	485 ± 50	328 ± 60	−170 ± 150	SiC, ms	
2c-1c1	150	45.3 ± 3.5	985 ± 150	228 ± 45	195 ± 235	SiC, ms	
2c-1c2	200	121 ± 4	−255 ± 25	293 ± 20	−70 ± 60	*Carbonaceous*	O, C
(b) C-anomalous grains from MET 00426							
2-3c1	330	54.1 ± 2.0	665 ± 60	n.m.	n.m.	SiC, ms	
2a-5c1	190	47.0 ± 1.5	915 ± 60	n.m.	n.m.	*SiC, ms*	
2b-11c1	200	29.1 ± 1.6	2100 ± 170	n.m.	n.m.	SiC, ms	
2b-12c1	150	124 ± 6	−275 ± 35	n.m.	n.m.	*Carbonaceous*	O, C
2b-14c1	200 × 150	120 ± 4	−250 ± 20	n.m.	n.m.	Carbonaceous	C, O
2b-14c2	280 × 310	58.4 ± 2.5	540 ± 65	n.m.	n.m.	*SiC, ms*	
2b-17c1	190	27.3 ± 0.7	2300 ± 95	n.m.	n.m.	*SiC, ms*	
2c-3c1	220	54.7 ± 3.2	645 ± 95	n.m.	n.m.	*SiC, ms*	
2c-8c1	220	108 ± 3	−170 ± 20	n.m.	n.m.	Carbonaceous	C, O
2c-9c1	180	115 ± 4	−220 ± 30	n.m.	n.m.	Carbonaceous	C, O
2d-5c1	180	136 ± 8	−340 ± 40	n.m.	n.m.	Carbonaceous	C, O
2d-9c1	190	44.7 ± 3.0	1015 ± 135	n.m.	n.m.	*SiC, ms*	
2d-10c1	190	5.1 ± 0.1	16, 670 ± 210	n.m.	n.m.	SiC, A+B	
4b-7c1	250	123 ± 7	−265 ± 45	n.m.	n.m.	SiC, Y	
4b-17c1	190	22.9 ± 0.9	2935 ± 155	n.m.	n.m.	SiC, ms	
4b-18c1	400	102 ± 1	−120 ± 10	n.m.	n.m.	*Carbonaceous*	n.m.
4b-20c1	250	135 ± 8	−335 ± 40	n.m.	n.m.	Carbonaceous	C, O, (N)
4c-6c1	570	109 ± 2	−170 ± 20	n.m.	n.m.	*Carbonaceous*	O, C
1a-4c1	240	57.2 ± 2.4	575 ± 65	280 ± 27	−30 ± 95	SiC, ms	
1a-15c1	190	75.2 ± 3.4	200 ± 55	328 ± 51	−170 ± 130	SiC, ms	
1a-17c1	380 × 200	107 ± 3	−155 ± 25	356 ± 15	−235 ± 35	Carbonaceous	C, O, N
1a-19c1	190	54.4 ± 2.4	655 ± 75	240 ± 39	135 ± 185	SiC, ms	
1c-3c1	100	68.1 ± 3.6	320 ± 70	367 ± 107	−260 ± 215	SiC, ms	
5a-1c1	150	54.0 ± 2.6	665 ± 80	257 ± 27	60 ± 115	*SiC, ms*	n.m.
5a-4c1	230	69.2 ± 3.2	300 ± 60	501 ± 56	−455 ± 60	*SiC, ms*	n.m.
5a-8c1	200	62.7 ± 2.8	435 ± 65	456 ± 476	−405 ± 620	SiC, ms	
5a-8c2	230	66.1 ± 2.8	360 ± 55	312 ± 147	−130 ± 410	SiC, ms	
5b-2c1	160	16.8 ± 0.9	4375 ± 280	281 ± 133	−35 ± 455	SiC, ms	
5b-6c1	490	79.1 ± 1.0	140 ± 15	167 ± 8	630 ± 75	C nanoglobule	C, O, (N)
5b-7c1	160	24.1 ± 1.0	2735 ± 150	224 ± 35	210 ± 185	*SiC, ms*	

Table 1
(Continued)

Grain	Size (nm)	$^{12}C/^{13}C$	$\delta^{13}C$[a]	$^{14}N/^{15}N$	$\delta^{15}N$[a]	Phase[b]	Elements[c]
5b-7c2	210	69.0 ± 1.5	305 ± 25	219 ± 11	245 ± 65	SiC, ms	
5b-8c1	270	60.2 ± 2.5	495 ± 60	275 ± 43	−10 ± 155	SiC, ms	
5b-9c1	160	66.0 ± 2.3	365 ± 50	506 ± 88	−460 ± 95	SiC, ms	
6e-8c1	200	125 ± 8	−280 ± 45	264 ± 35	30 ± 135	*SiC*, *Y*	
6e-12c1	500 × 250	5.9 ± 0.1	14, 280 ± 250	255 ± 12	65 ± 50	SiC, A+B	

Notes.
[a] Deviation from normal in parts per thousand: $(R_{meas}/R_{std}-1) \times 1000$.
[b] ms = mainstream: grains in italics are those for which the identification is less certain (see the text for details).
[c] Elements are shown only for carbonaceous grains and are listed in order of abundance: parentheses indicate that an element was detected in elemental maps, but was not observed above noise levels in spectra (n.m. = not measured).

We used the Auger Nanoprobe to obtain SE images of the grains and to determine their compositions. The C-anomalous grains can be broadly sub-divided into two groups: carbonaceous grains and SiC grains (Table 1). The carbonaceous grains generally appear dark in SE images with irregular shapes and their Auger spectra are dominated by C, although O is usually also present; N is found in some of these grains as well. In contrast, SiC grains are typically light-colored in SE images and are sometimes hard to distinguish from the surrounding matrix material. As expected, their Auger spectra are dominated by C and Si, although some O is often also present (see above). Below we discuss each of these groups in more detail.

3.1 SiC Grains

A total of 41 SiC grains were identified through a combination of NanoSIMS ion images, Auger electron energy spectra, and Auger elemental mapping. 12 grains are listed in italics in Table 1, indicating that their identification is somewhat uncertain. In all but three cases this is because the grains had sputtered away during the NanoSIMS measurement and, therefore, could not be measured in the Auger Nanoprobe. The remaining three grains (5c-18c1 from QUE 99177, and 2a-5c1 and 6e-8c1 from MET 00426) could not be located after the NanoSIMS measurements because of difficulties with the sample surfaces in the areas of the measurements (e.g., formation of cracks after the SIMS measurements which precluded proper alignment of the Auger and NanoSIMS SE images). The tentative identification of these grains as SiC thus rests largely on their isotopic compositions, as well as estimates of their Si/C ratios obtained from the NanoSIMS ion images (when measured, i.e., in the C and N imaging series). The latter can vary considerably, depending on the measurement conditions; $^{28}Si^-/^{12}C^-$ ratios for SiC grains are fairly uniform ($\leqslant$20% variation) within a given measurement set, but varied by as much as a factor of 3 for measurements done at different times and in different matrix areas, due to variations in the setup of the detector used to monitor $^{28}Si^-$. However, this ratio is consistently significantly higher (usually by close to an order of magnitude) in SiC grains than in carbonaceous grains and, therefore, is reasonably diagnostic. Figure 2 illustrates this point: C and N isotopic ratio images (expressed in delta notation), along with the $^{12}C^-$ and $^{28}Si^-$ ion images, are shown for C-anomalous grain 5b-9c1 from MET 00426. The grain is readily identified as a mainstream SiC on the basis of its C and N isotopic compositions (see below) and its high Si signal. Whenever possible the SiC grains from the C and N imaging measurements were also analyzed by Auger Nanoprobe in order to verify these identifications.

We note, however, that $^{28}Si^-$ was not measured during the C and O NanoSIMS imaging searches and, therefore, SiC grains from this set of measurements could be identified only through Auger analysis. Figure 3 shows SE images of three SiC grains, along with Auger spectra and/or elemental maps used to identify the grains. Grains 5b-7c2 and 5b-8c1 from MET 00426 are both mainstream SiC grains that are about 200 nm in diameter. The Auger spectrum of 5b-7c2 in Figure 3(a) shows that, as noted earlier, some O is often present in the spectra of these grains in addition to Si and C. Note that the peak appears large because O is very sensitive in the Auger Nanoprobe, but that the amount of O present comes to only ∼15 at.% when quantified. From Figure 3(b) it is clear that SiC grains can also be identified from Auger elemental maps on the basis of correlated high abundances of C and Si and low abundances of O. Figure 3(c) shows a SiC grain of type A+B, with a $^{12}C/^{13}C$ ratio of 6 and a normal N isotopic composition. This grain is about 500 nm long and 200 nm wide, and contains a section protruding from one end that may be part of the same grain or could be a separate adjacent SiC grain. The NanoSIMS measurement only imaged the left edge of the grain and, thus, the isotopic data do not provide information about whether this is one homogeneous SiC or two different grains.

Finally, some SiC grains were particularly hard to identify due to their small size. Figure 4 shows one of these grains. The grain, 7b-2c1 from QUE 99177, is difficult to distinguish in the SE image, and NanoSIMS ion images show a low $^{12}C^-$ signal, although it is clearly visible in the $^{13}C^-$ image. By comparing the NanoSIMS ion images with the Auger elemental maps, we were able to establish that the grain corresponds to the circled region shown in Figure 4, which contains both C and Si, but is depleted in O. Together with its low $^{12}C/^{13}C$ ratio of 19, these data indicate that this grain is most probably a SiC.

The morphologies and sizes of the SiC grains found in situ in QUE 99177 and MET 00426 are generally similar to presolar SiC grains obtained from acid residues (Amari et al. 1994) and physically disaggregated pristine SiC (Bernatowicz et al. 2003). Our grains have sizes ranging from 150 to 500 nm, which is consistent with previous data indicating that most presolar SiC is less than 0.5 μm in size (Zinner 2004). Disaggregated SiC grains exhibit a variety of morphologies; many are platy and roughly equant with hexagonal or triangular shapes (Amari et al. 1994). Although some grains are euhedral with well-developed crystal faces (Bernatowicz et al. 2003) most are, in fact, subhedral (Amari et al. 1994; Bernatowicz et al. 2003). This variety is reflected in our grains as well. Most of our grains are subhedral and equant (e.g., Figure 3(b)), but we also see occasional euhedral grains with obvious crystal faces

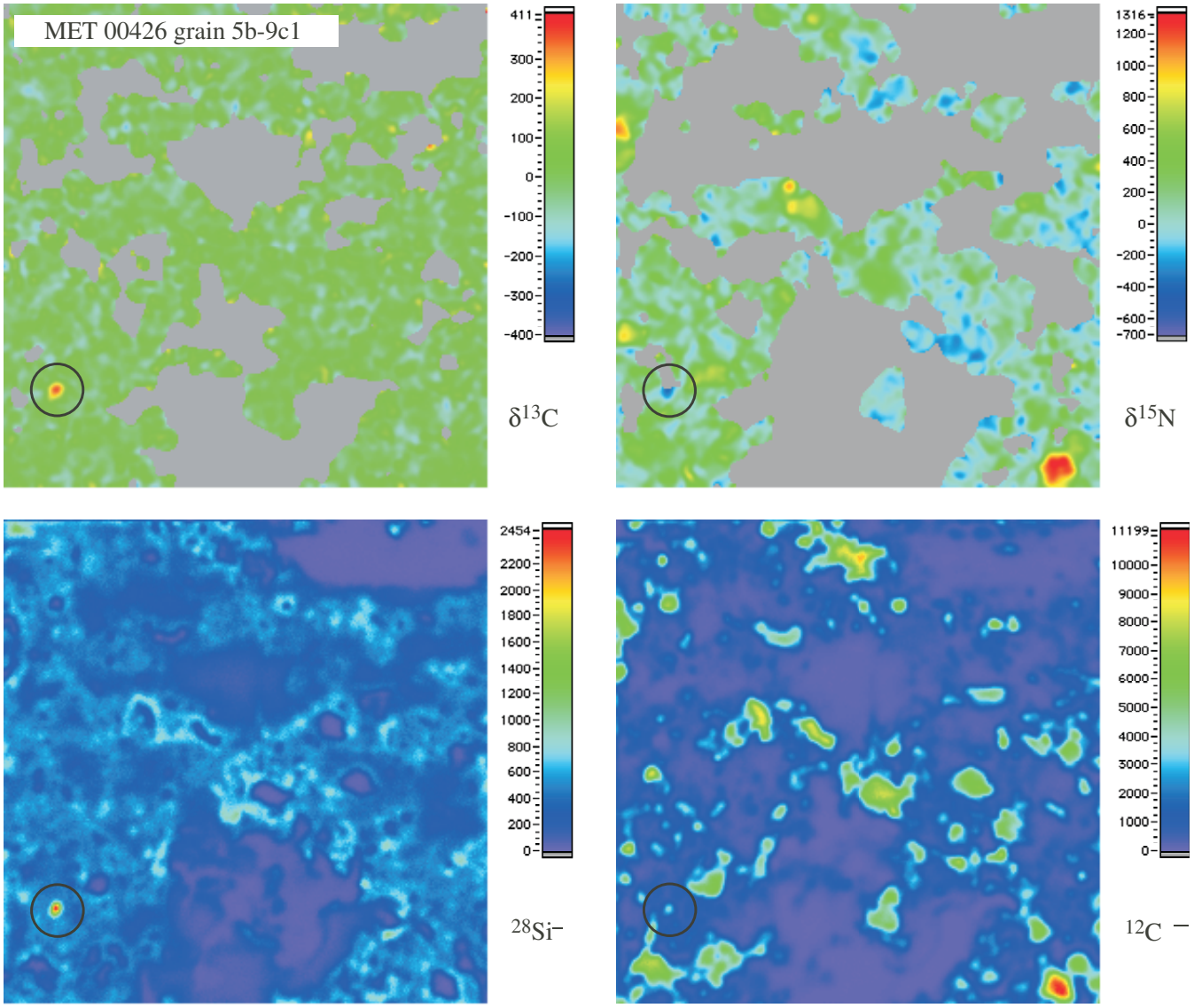

Figure 2. NanoSIMS false color images of area 5b-9 from MET 00426, showing C and N isotopic compositions (δ^{13}C and δ^{15}N), and C and Si elemental distributions. Mainstream SiC grain 5b-9c1 is circled in black. Field of view is 10 μm.

(e.g., Figure 3(a)) and grains with unusual morphologies (e.g., Figure 3(c)).

Based on their ^{12}C/^{13}C ratios, between 17 and 82, almost all of the SiCs (37 of 41) can be classified as mainstream grains (Table 1, Figure 1(a)). Most mainstream grains from acid residue studies are enriched in ^{14}N, but the measurements from this study mostly show terrestrial ^{14}N/^{15}N ratios. This is likely due to the low intrinsic N abundances of the grains and contributions from isotopically normal N from the surrounding matrix material. In contrast, most acid residue SiCs have been measured as isolated grains on high purity Au foils, resulting in less contamination from isotopically normal N. Two grains have ^{12}C/^{13}C ratios of less than 10 and, thus, appear to be A+B grains, and the final two grains may be Y grains, with ^{12}C/^{13}C ratios of >100. The relative abundances of the different SiC grain types are roughly consistent with the distribution expected from past work on acid residues (Zinner 2004). We have not identified any SiC X grains in our work. However, without Si isotopic data, we cannot completely exclude the possibility that some of the mainstream grains whose N isotopes were not measured may in fact be X grains. We note though that X grains make up only 1% of the population of SiC grains and, although their ^{12}C/^{13}C ratios can be lower than solar, most exhibit excesses rather than depletions in ^{12}C (Zinner, 2004). Similarly, one of the Y grains for which we have no N isotopic data could also be an X grain.

Mainstream grains, which are defined by ^{12}C/^{13}C ratios between 10 and 100, and make up ~93% of all SiC (Zinner 2004), are generally thought to have originated in AGB stars that have undergone the third dredge-up, resulting in C/O ratios of greater than 1, which causes the star to become a carbon star (e.g., Zinner, 2004; Lodders & Amari 2005). The ^{13}C and ^{14}N excesses observed in mainstream SiC are the result of hydrogen burning via the CNO cycle during the main-sequence phase of the star. This material is brought to the surface of the star during the first and second dredge-ups and is mixed with ^{12}C produced by shell He burning during the AGB phase, leading to a range of ^{12}C/^{13}C ratios from about 20 to 200 and ^{14}N/^{15}N ratios up to about 1600 (Hoppe & Ott 1997). Extra mixing of envelope material ("cool bottom processing"; Wasserburg et al. 1995) to deep regions close to the H-burning shell has been invoked to account for the higher ^{14}N/^{15}N ratios actually observed in mainstream SiC grains (Hoppe & Ott 1997; Zinner

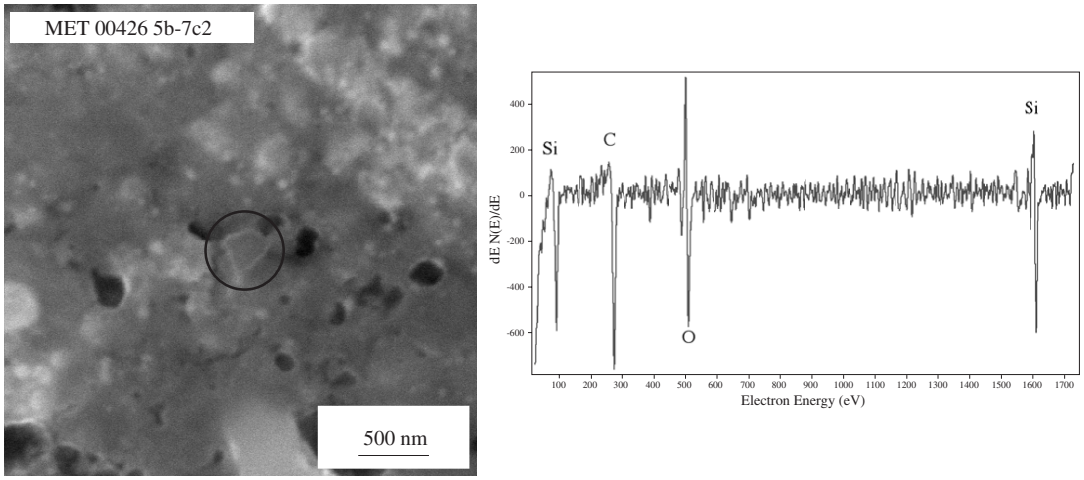

(a)

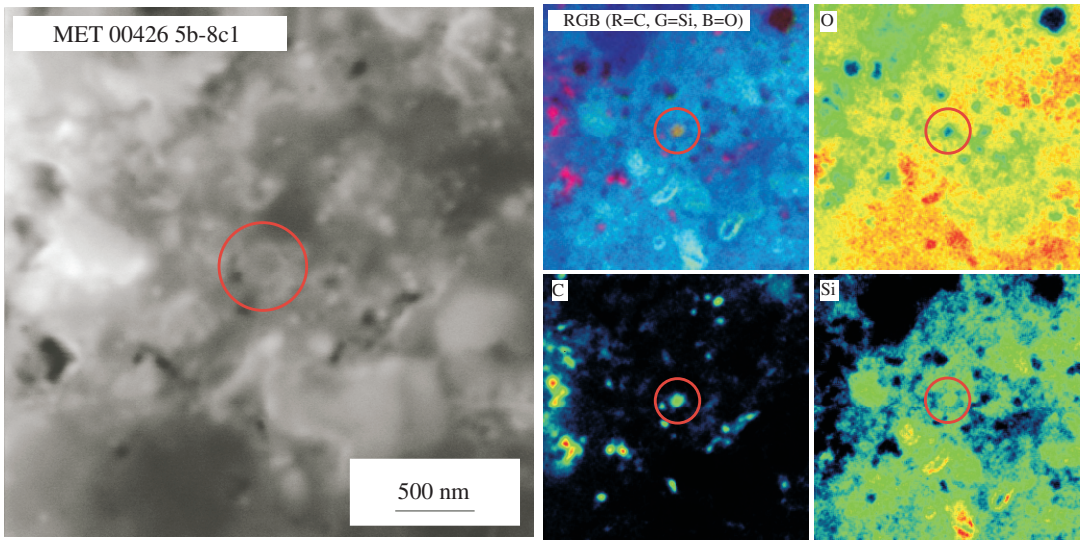

(b)

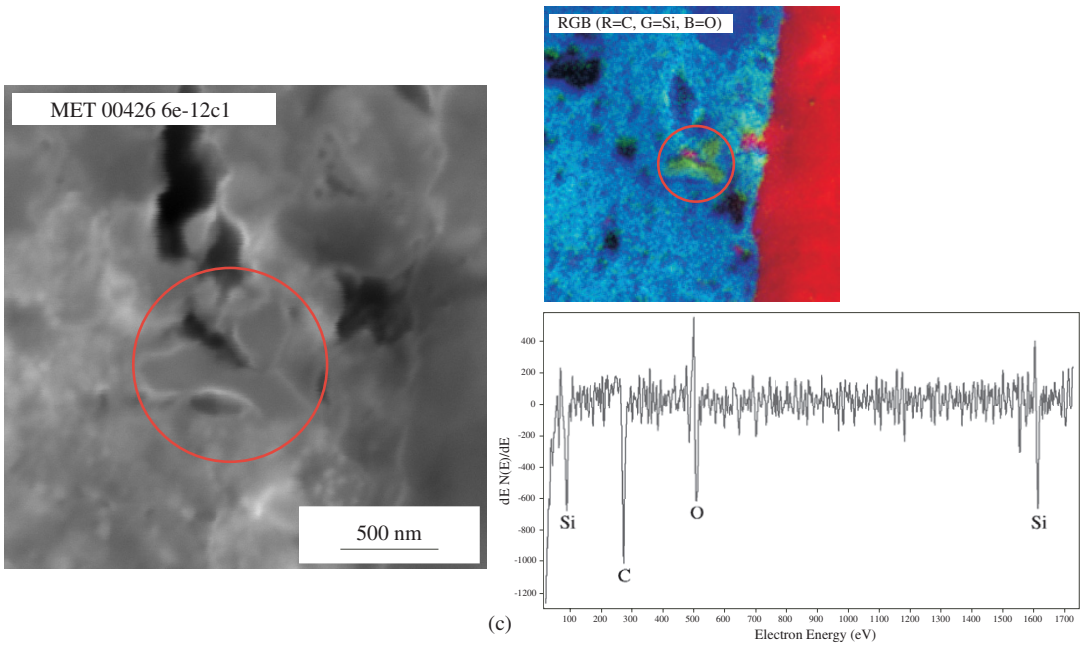

(c)

Figure 3. (a) Secondary electron image and differentiated Auger electron energy spectrum of mainstream SiC grain 5b-7c2 (circled in black) from MET 00426. (b) Secondary electron image and false color Auger elemental distribution maps of mainstream SiC grain 5b-8c1 (circled in red) from MET 00426. (c) Secondary electron image, false color Auger elemental distribution map, and differentiated Auger electron energy spectrum of type A+B SiC grain 6e-12c1 (circled in red) from MET 00426. Note that the edge of the NanoSIMS presputter area is visible on the right of the SE image and that the portion of the grain imaged in the NanoSIMS is the 100 nm inside the left edge of the red circle.

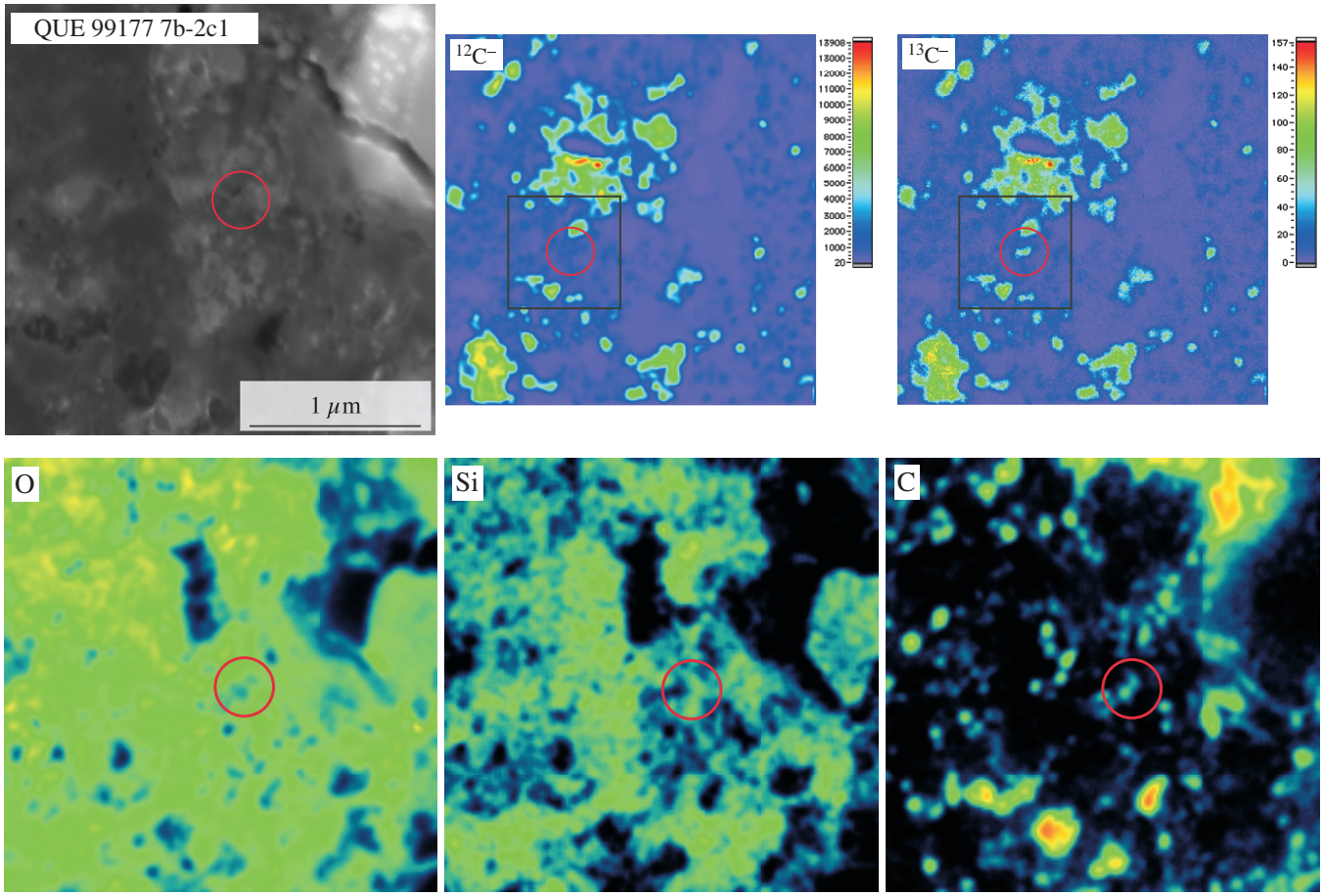

Figure 4. Secondary electron image and false color Auger elemental distribution maps and NanoSIMS ion images of mainstream SiC grain 7b-2c1 (circled in red) from QUE 99177. The $^{13}C^-$ distribution defines the isotopic anomaly of this grain. The black boxes in the ion images outline the approximate area shown in the SE and elemental images.

2004). The Si isotopic compositions of mainstream SiC grains are characterized by enrichments in the heavy isotopes and, in a three-isotope Si plot, fall along a line of slope 1.4 that is shifted slightly to the right of the solar composition (see Figure 4 of Zinner 2004).

Two of the SiC grains from this study are probable Y grains. These grains make up ∼1% of the SiC population and are characterized by $^{12}C/^{13}C$ ratios of >100 and Si isotopic compositions that fall to the right of the mainstream SiC correlation line in a three-isotope plot. These grains also have an AGB origin, but the isotopic data, including Si and Ti isotopic ratios, indicate an origin in stars with metallicities that are lower than solar ($Z \sim 0.01$; Amari et al. 2001a). Finally, two SiC grains belong to the group A+B, which make up about 4%–5% of all SiC grains. These grains have $^{12}C/^{13}C$ ratios of <10 and about 1/3 of the grains have $^{14}N/^{15}N$ ratios that are lower than the terrestrial value; the Si and Ti isotopic ratios of such grains are similar to those observed in mainstream SiC grains. The origin of A+B grains is unclear and it is possible that they come from more than one source. Both J-type carbon stars and born-again AGB stars (e.g., Sakurai's object) have been proposed, but neither source can adequately account for the low $^{14}N/^{15}N$ ratios observed in some of these grains (Amari et al. 2001b).

3.2 Carbonaceous Grains

The remaining 28 anomalous areas (Figure 1(b)) have compositions dominated by C and appear to be some type of carbonaceous matter. These often appear as dark irregular grains in SE images and tend to be somewhat larger than most of the SiC grains, although all are less than 1 μm in size (Table 1). A few of the regions look more like diffuse C-enriched areas than like discrete compact grains (Figure 5). The corresponding C isotopic anomalies also appear to be rather patchy and to some extent resemble diffuse ^{15}N-enriched areas seen in IDPs and IOM from primitive meteorites (Floss et al. 2006; Busemann et al. 2006a). Although these are not technically discrete grains, for convenience we refer to all anomalous carbonaceous areas as grains in the text. As is the case for some SiC grains, 12 carbonaceous grains are listed in italics, indicating a somewhat uncertain identification. Seven grains could not be measured in the Auger Nanoprobe either because they had sputtered away or because of sample charging issues in the vicinity of the grains. Five of these grains were identified in the C and N imaging series and have very low $^{28}Si^-/^{12}C^-$ ratios, indicating that they are most likely carbonaceous. Ratios of $^{16}O^-/^{12}C^-$ are also low for the two grains measured in the C and O imaging series, again suggestive of carbonaceous material. The remaining five grains that are highlighted with italics in Table 1 have Auger spectra in which the abundance of O appears to be greater than the abundance of C; although these grains also have $^{28}Si^-/^{12}C^-$ and $^{16}O^-/^{12}C^-$ ratios that are low, we have flagged these grains as having uncertain compositions.

Auger Nanoprobe measurements show that the spectra of carbonaceous grains are dominated by high C abundances (Figure 6). Oxygen is often also present, but, as discussed earlier,

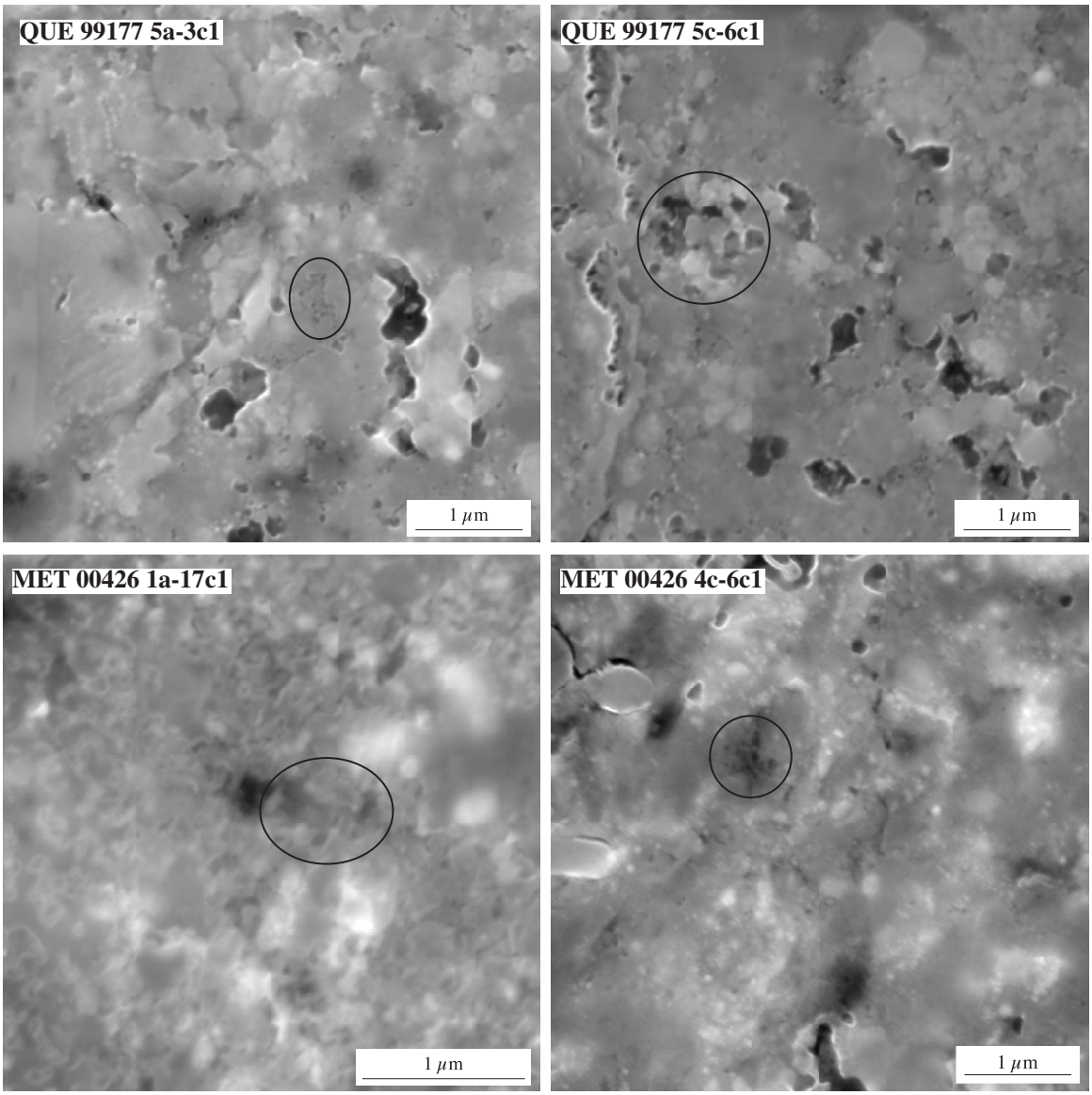

Figure 5. Secondary electron images of isotopically anomalous carbonaceous regions from QUE 99177 and MET 00426.

it is not clear whether it is part of the grains' compositions or is the result of an external contribution. Quantification of the Auger spectrum shown in Figure 6 suggests that grain 5a-7c1 from QUE 99177 consists of 92 at.% C and 8 at.% O, if the PHI pure element-based sensitivity factors (Childs et al. 1995) can be used and if the O present is indeed intrinsic to the grain. Some of the carbonaceous grains also contain N. The Auger elemental maps of grain 5b-3 from QUE 99177 (Figure 7) show that N in this grain is correlated with C; the Auger spectrum in this case exhibits a distinct N peak. Nitrogen is not very sensitive in the Auger Nanoprobe and the peak is barely above the noise level. Quantification of the spectrum, using a sensitivity factor for N determined from a Si_3N_4 standard suggests a N concentration of 8 at.% in this grain. However, Si_3N_4 may not be the most appropriate standard for determining N abundances in carbonaceous matter and this value should be considered preliminary; work is currently underway to obtain sensitivity factors from more appropriate phases, such as kerogens. Only three carbonaceous grains have N abundances that are detectable above the background noise levels of the Auger spectra; another five grains show evidence in elemental maps for the presence of N correlated with C in the grains, but do not contain enough N to detect in their Auger spectra (Table 1).

One grain, 5b-6c1 from MET 00426, appears to be a C nanoglobule of the type recently identified in the Tagish Lake (Nakamura-Messenger et al. 2006) and Bells (Messenger et al. 2008) carbonaceous chondrites (Figure 1(b)). The grain, which is enriched in ^{13}C and ^{15}N, is about 500 nm in diameter with a distinct hole in the center (Figure 8). Auger elemental maps show that it contains some N, in addition to C. Quantification of the Auger spectrum of this grain suggests ~3 at.% N, but the lack of a distinct peak above noise level indicates that this must be considered an upper limit.

Almost all of the carbonaceous grains have $^{12}C/^{13}C$ ratios that are higher than normal terrestrial values (101–136). Only three grains (in addition to the C nanoglobule, which is considered separately below) have ^{13}C-enriched compositions (Table 1, Figure 1(b)). Nitrogen isotopic compositions in these grains tend to be anomalous and there is a distinct subgroup of grains that exhibit enrichments in ^{15}N (Figure 1(b)) similar in magnitude to the enrichments commonly observed in ^{15}N-rich hotspots in IDPs (Floss et al. 2006) and in insoluble organic matter from

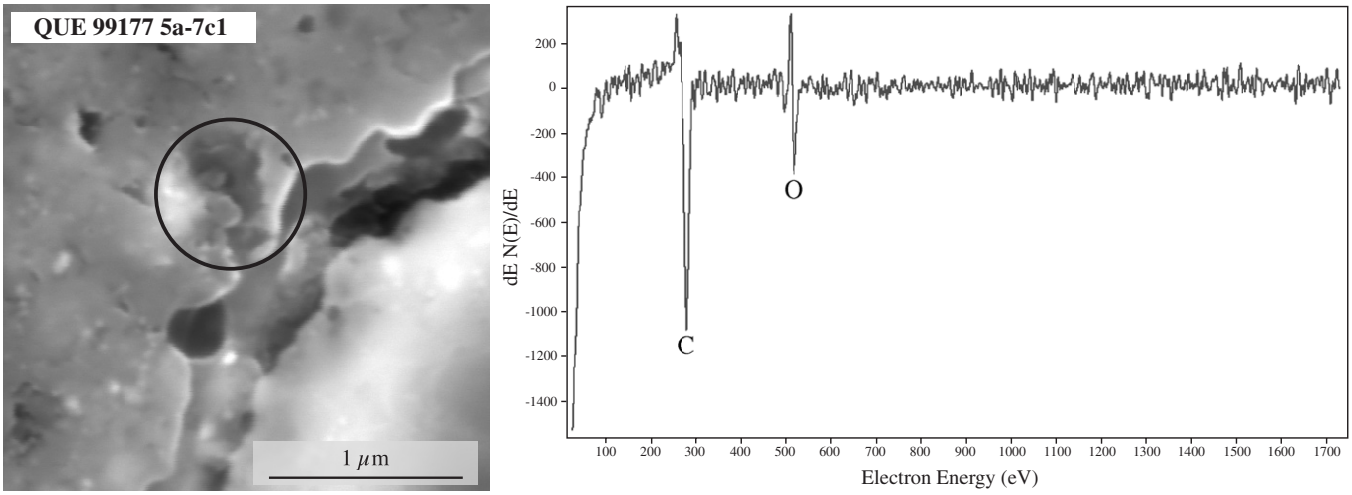

Figure 6. Secondary electron image and differentiated Auger electron energy spectrum of carbonaceous grain 5a-7c1 (circled in black) from QUE 99177.

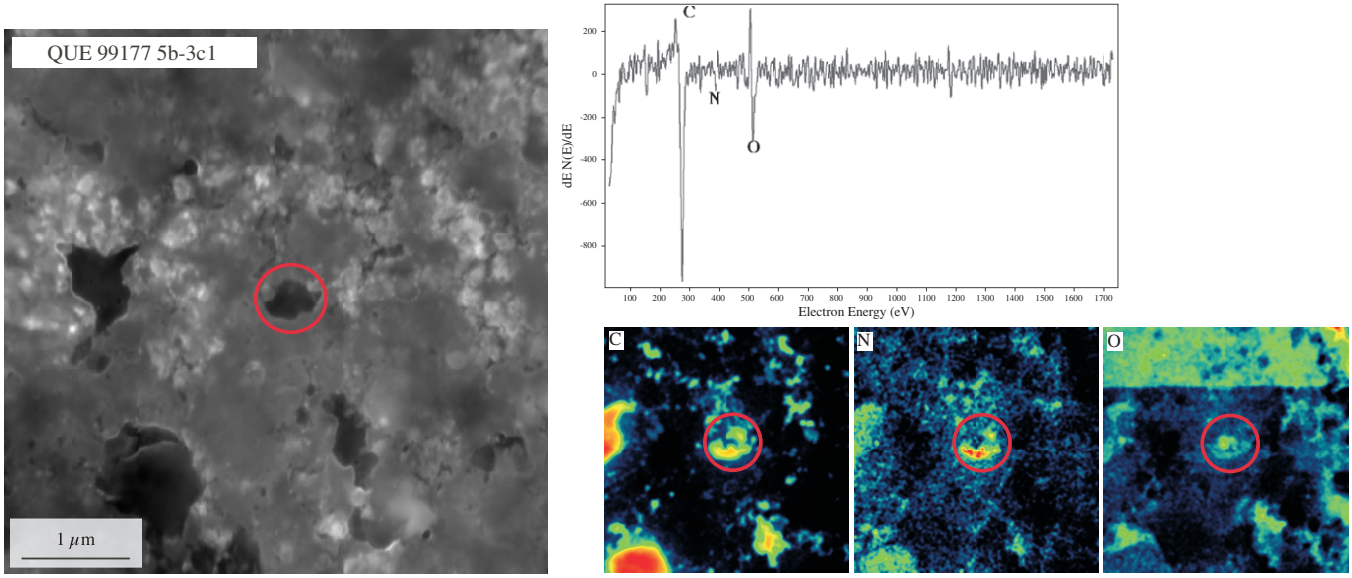

Figure 7. Secondary electron image, false color Auger elemental distribution maps, and differentiated Auger electron energy spectrum of carbonaceous grain 5b-3c1 (circled in red) from QUE 99177.

primitive meteorites (Busemann et al. 2006a). Both QUE 99177 and MET 00426, like other CR chondrites, exhibit abundant N isotopic anomalies in addition to the C-anomalous grains discussed here, with average bulk enrichments up to $\delta^{15}N = \sim 500$ ‰ and individual ^{15}N-rich hotspots with up to $\delta^{15}N = \sim 2475$ ‰ (Floss & Stadermann 2009b); these N isotopic anomalies are not accompanied by C isotopic anomalies and will be the topic of a future paper.

In principle, it is possible that some of the carbonaceous grains identified here could be graphite. Presolar graphite grains have a wide range of $^{12}C/^{13}C$ ratios, but many grains show ^{12}C excesses like the grains from our study (Zinner 2004). Nitrogen isotopic ratios are normal in most graphite grains (Hoppe et al. 1995; Zinner et al. 1995; Jadhav et al. 2006), although this is generally attributed to isotopic equilibration, given the large range in C isotopic ratios. Low-density graphite grains are an exception, however, and exhibit anomalous N isotopic compositions (Zinner 2004), with enrichments in ^{15}N like those observed in our carbonaceous grains. Low-density graphites also exhibit anomalies in O and Si, and have high $^{26}Al/^{27}Al$ ratios (e.g., Jadhav et al. 2006). Silicon and Mg–Al isotopic data are not available for our grains, but we do have O isotopic data for those carbonaceous grains that were identified in the C and O imaging series. These data indicate normal O isotopic compositions for all the carbonaceous grains measured, with no indication of the ^{18}O enrichments seen in low-density graphites (Zinner 2004), suggesting that most of our carbonaceous grains are probably not graphite. Moreover, studies have shown that circumstellar graphite grains are generally round and that graphite grains that are not round have normal C isotopic compositions (Amari et al. 1990; Zinner et al. 1995; Mostefaoui et al. 2005). As noted above, most of our grains have irregular shapes or resemble diffuse patchy regions (Figure 5), a further indication that they are not graphite. Ultimately we cannot definitively rule out that some graphite grains are present in our population of carbonaceous grains. However, both the morphologies and isotopic characteristics suggest that most of our grains are not presolar graphite.

It is more likely that these carbonaceous grains are related to C- and N-anomalous phases that have occasionally been observed in IDPs and in the IOM from some primitive meteorites. A total of three such grains have been found previously and

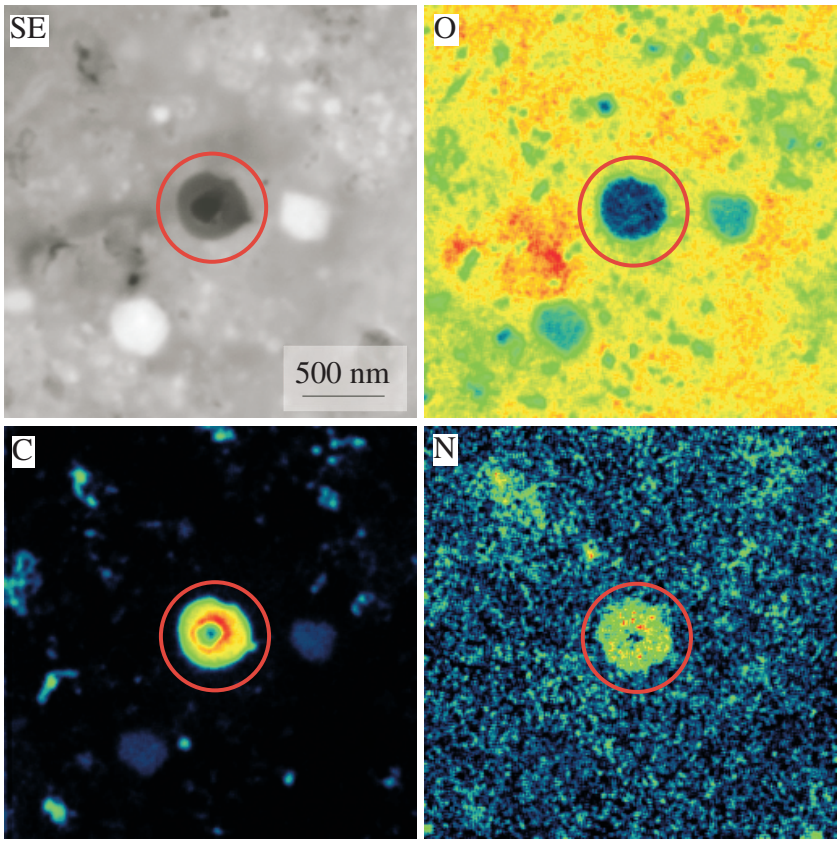

Figure 8. Secondary electron image and false color Auger elemental distribution maps of grain 5b-6c1 (circled in red) from MET 00426.

are shown in Figure 1(b). Two of the grains, one from the IDP Benavente (Floss et al. 2004) and one from IOM from the CR2 chondrite EET 92042 (Busemann et al. 2006b), have ^{12}C-rich and ^{15}N-rich isotopic compositions similar to the subset of ^{15}N-rich grains from this study. TEM analysis of focused ion beam (FIB) sections extracted from these grains showed that both consist of amorphous C-rich matter (Floss et al. 2004; Busemann et al. 2006c); IR spectra of the Benavente grain show a prominent C–H stretch feature consistent with those observed in aliphatic hydrocarbons, indicating that the material is organic in nature, and electron energy loss spectroscopy suggests the presence of 1–2 wt.% N (Floss et al. 2004). A third grain found in the IDP Hesse (Floss et al. 2006) is also ^{15}N-enriched, but shows an excess rather than a depletion of ^{13}C (Figure 1(b)). Preliminary TEM analysis of a FIB section extracted from this grain showed that the area was very C-rich; unfortunately, the section was lost before additional measurements could be carried out. With a few exceptions noted in italics in Table 1, the carbonaceous grains from this study that were analyzed by Auger Nanoprobe are all very C-rich. Some grains also show detectable (several at.%) amounts of N in their Auger spectra; Auger elemental mapping shows the presence of minor N in a few additional grains, although abundances are within the noise level of the Auger spectra.

As discussed at length by several authors (Messenger & Walker 1997; Alexander et al. 1998; Floss et al. 2004, 2006) H, N, and C isotopic anomalies commonly observed in primitive materials, such as IDPs and the CR chondrites, are generally thought to originate in cold molecular clouds. Theoretical studies of low-temperature interstellar chemistry show that ^{15}N enhancements can be produced through ion–molecule exchange reactions involving common N-bearing species in interstellar clouds. Early work suggested enrichments on the order of 250‰ (Terzieva & Herbst 2000), significantly less than the maximum enhancements observed in IDPs and primitive meteorites (Floss et al. 2006; Busemann et al. 2006a), but more recent work focusing on NH_3 formation in dense molecular clouds (Rodgers & Charnley 2008) indicates that enrichments of more than 3000‰ are possible at very low temperatures ($T < 10$K). These values are sufficient to account for the ^{15}N-rich hotspots found in extraterrestrial materials. Gas-phase reactions are also expected to produce C isotopic fractionations, but different processes produce competing fractionations (e.g., Langer et al. 1984; Langer & Graedel 1989; Sandford et al. 2001). Indeed, the existence of multiple reaction pathways, which might act to cancel out the anomalies produced, has been suggested as one reason for the relative scarcity of C isotopic anomalies in primitive extraterrestrial materials (Tielens 1997; Sandford et al. 2001). However, the high abundance of carbonaceous grains with C isotopic anomalies found in this study suggests instead that secondary processes are responsible for the low abundances often observed (see Section 3.4).

As noted originally by Floss et al. (2004), the presence of C isotopic anomalies associated with heteroatomic organic compounds indicates that this carbonaceous material is itself of presolar interstellar origin, rather than simply being a more recent solar system host substrate for the D and N enrichments commonly observed in IDPs and the IOM of primitive meteorites. Experimental work shows, furthermore, that icy interstellar analogs can be easily converted to complex organic compounds through UV photolysis (Bernstein et al. 2002, 2003). However, the presence of associated C and N isotopic

anomalies may not require processes that can produce both effects in the same material, as suggested by Floss et al. (2004), if ^{15}N enrichments are inherited from isotopically fractionated ammonia ice mantles (Rodgers & Charnley 2008). Moreover, the presence of both ^{13}C-enriched and ^{13}C-depleted grains in our study indicates that a variety of reactions do contribute to the formation of interstellar carbonaceous material. Finally, because ^{15}N-enriched hotspots without associated C isotopic anomalies are also common in QUE 99177 and MET 00426, just as they are in other extraterrestrial materials, reactions that do not strongly fractionate ^{12}C from ^{13}C must also be important in low temperature interstellar chemistry. Indeed, Langer & Graedel (1989) note that there is little isotopic fractionation for CO and HCO^+ and that fractionations for other carbon species are highly sensitive to the physical conditions present.

3.3 Nanoglobules in Extraterrestrial Materials

One of the C-anomalous grains found in MET 00426 consists of a round C-rich spherule with a hollow interior that strongly resembles organic nanoglobules recently reported from a variety of primitive meteorites, IDPs, and cometary matter (Nakamura-Messenger et al. 2006; Messenger et al. 2008; Garvie et al. 2008; De Gregorio et al. 2008). Although the existence of these objects has been known for some time (Claus & Nagy 1961), their origin as likely products of low-temperature interstellar chemical reactions has only recently been established. Abundant nanoglobules have been found in the Tagish Lake and Bells carbonaceous chondrites and are generally characterized by elevated D/H ratios, up to nine times the terrestrial value, and ^{15}N enrichments up to ~1000‰; the grains are composed of amorphous carbon, lacking any long-range order of graphitic structure (Nakamura-Messenger et al. 2006; Messenger et al. 2008). The N isotopic composition of the nanoglobule from MET 00426 is within this range, with a δ^{15}N of 630‰ ± 75‰ (Table 1). However, this is the first reported nanoglobule with a C isotopic anomaly (δ^{13}C = 140‰ ± 15‰). Nakamura-Messenger et al. (2006) have speculated that these nanoglobules formed in cold molecular clouds as ultraviolet radiation converted simple ices formed on grain surfaces into more complex refractory organic compounds. Volatilization or aqueous alteration of more labile interior ices may account for the hollow cores observed in many of these globules. Although most of the nanoglobules found by Nakamura-Messenger et al. (2006) have hollow spherical structures like the globule from this study (Figure 8), Garvie et al. (2008) note that some nanoglobules are solid grains, and that aggregate clustered and intergrown particles in fact dominate the nanoglobule population in Tagish Lake; however, the globules from that study were not analyzed for their isotopic compositions and it is, therefore, unclear if their origin is similar to those studied by Nakamura-Messenger et al. (2006). Aggregate nanoglobules with irregular shapes containing D and ^{15}N enrichments are, however, found in the Bells CM2 chondrite (Messenger et al. 2008). It is possible that some of our irregular carbonaceous grains are also aggregate nanoglobules; however, detailed morphological information is difficult to extract from the SE images of our in situ grains and TEM analyses would likely be required to evaluate whether this is the case. In addition, the distinction between nanoglobules and other interstellar carbonaceous matter may be largely academic, as both types of grains probably have similar origins: isotopic compositions have similar reported ranges and, although we do not have structural information about the C-anomalous grains from this study, as we noted above, two of the three interstellar carbonaceous grains previously reported from IDPs and primitive meteorites also consist of heteroatomic amorphous carbon (Floss et al. 2004; Busemann et al. 2006c).

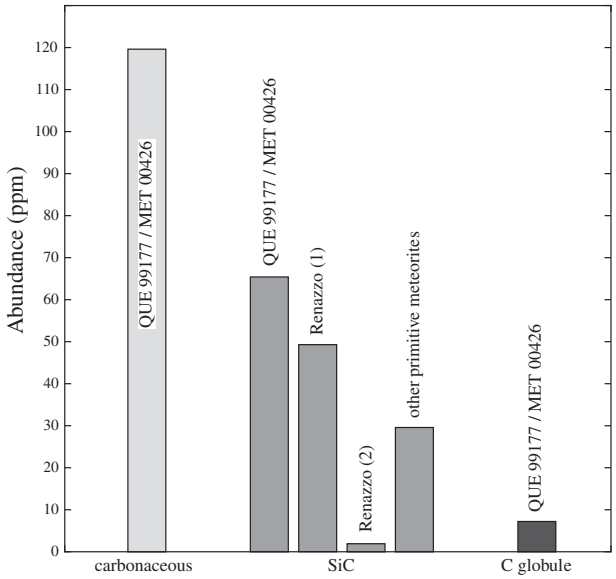

Figure 9. Plot of the abundances of C-anomalous phases in QUE 99177 and MET 00426. For SiC, comparison abundances are shown for other primitive meteorites (Zinner 2004) and Renazzo (data for (1) are from Floss & Stadermann 2005 and for (2) are from Huss et al. 2003).

3.4 Abundances of C-anomalous Grains

The 69 C-anomalous grains (both SiC and carbonaceous) were found within 15,400 μm^2 and 12,900 μm^2 of matrix material from QUE 99177 and MET 00426, resulting in matrix-normalized abundances of 215 ± 35 ppm and 175 ± 30 ppm (1σ errors are based on counting statistics only and should be considered lower limits), respectively, for these meteorites. These abundances are similar to those calculated for O-anomalous grains from these two meteorites (160–220 ppm; Floss & Stadermann 2009a) and are significantly higher than estimates of the abundances of presolar carbonaceous phases (except for nanodiamonds) in other meteorites (e.g., Zinner 2004). Below we discuss the distribution of the C-anomalous grains in more detail.

Based on the single confirmed C nanoglobule identified here, we calculate an abundance of 8^{+18}_{-6} ppm (1σ errors after Gehrels 1986) in the two CR3 chondrites (Figure 9). However, as noted above, some of the other C-anomalous carbonaceous grains could also be nanoglobules. Moreover, both QUE 99177 and MET 00426 contain abundant ^{15}N-rich hotspots (Floss & Stadermann 2009b). Although we have not yet identified the carrier phases of these anomalies, examination of the NanoSIMS ion images suggests that many of them are likely candidate nanoglobules. Thus, the true abundance of nanoglobules in these two CR3 chondrites is almost certainly significantly higher than the number listed here.

The calculated abundance of SiC grains in QUE 99177 and MET 00426 is 65 ± 10 ppm (Figure 9); SiC is about a factor of 2 more abundant in MET 00426 than in QUE 99177 (~90 vs. ~45 ppm). The average abundance for both meteorites is about a factor of 2 higher than the maximum SiC abundances previously observed in other primitive meteorites (Zinner, 2004), but compares well (within the relatively large 1σ errors) to a separate estimate of 50^{+90}_{-30} ppm for the CR2

chondrite Renazzo based, like this study, on in situ ion imaging of C isotopes (Floss & Stadermann 2005). In that work, two 300 nm SiC grains, identified on the basis of their Si/C ratios from NanoSIMS ion images, were found in 3560 μm^2 of matrix fragments separated from the Renazzo meteorite. Both grains appear to be mainstream SiC with ^{12}C/^{13}C ratios of 49 $\pm$ 1 and 23 $\pm$ 1; ^{14}N/^{15}N ratios are 466 $\pm$ 54 and 275 $\pm$ 49, respectively. Both of these abundance estimates are significantly higher than a value of $\sim$2 ppm for SiC in Renazzo calculated by Huss et al. (2003), based on the determination of the noble gas contents of acid residues. A recent ion imaging study to search for SiC in the insoluble organic matter from various primitive meteorites (Davidson et al. 2009) found matrix-normalized abundances of 25–55 ppm in CR1 and CR2 chondrites, comparable to the values calculated here for QUE 99177 and MET 00426. The lower abundances determined by Huss et al. (2003) could be due to degassing of SiC during thermal metamorphism or possibly the destruction of a small gas-rich fraction of SiC grains. Davidson et al. (2009) note that SiC abundances are similar in both CR2 and CR1 chondrites, indicating that the aqueous alteration experienced by these meteorites does not play a significant role in destroying SiC grains.

Most striking, however, is the high abundance of isotopically anomalous carbonaceous grains, about 120 $\pm$ 23 ppm in these CR3 chondrites (Figure 9). Estimates of the abundances of these grains in the EET 92042 CR2 chondrite are not available, but, with only one grain found (Busemann et al. 2006b), they appear to be much less common than observed in QUE 99177 and MET 00426 (see above and Figure 1(b)). In contrast, the abundance of such grains in isotopically primitive IDPs (Floss et al. 2004, 2006) appears to be similar to that observed in the CR3 chondrites. Although abundance estimates based on only two C-anomalous interstellar grains are rather uncertain, within 1σ errors the value of 420^{+765}_{-270} ppm calculated for isotopically primitive IDPs (Floss et al. 2006) is, in fact, consistent with the abundances calculated for the CR3 chondrites.

We note that the abundance estimate provided above for the CR3 chondrites only accounts for those grains that have anomalous C isotopic compositions; the actual abundance of all interstellar carbonaceous grains is significantly higher than this value, as the ^{15}N-rich hotspots in these meteorites most likely have an interstellar origin as well. The abundance of these grains has not been calculated (indeed it is difficult to do so, since there is no clear cutoff between localized hotspots and larger, more diffuse regions that have somewhat lower ^{15}N-enrichments), but we note that they are vastly more common in QUE 99177 and MET 00426 than grains with C isotopic anomalies. There is also a considerable difference in the abundance of C-anomalous carbonaceous grains between the two meteorites. The abundance in QUE 99177 is 170 $\pm$ 40 ppm, whereas it is only 60 $\pm$ 20 ppm in MET 00426. The bulk of the C-anomalous grains in QUE 99177 (12 of 18) come from matrix area 5 (Table 1) and, thus, the difference in abundance between the two meteorites is likely a sampling effect resulting from incorporation of this region in the imaging searches from QUE 99177. We have observed a similar heterogeneity in the distribution of O-anomalous grains in different matrix areas of QUE 99177 (Floss & Stadermann 2009a), with significantly higher abundances of presolar silicates/oxides in matrix area 5 (335 $\pm$ 75 ppm) compared to other matrix areas (90 $\pm$ 40 ppm). In addition, 10 of the 16 presolar SiC grains in QUE 99177 come from matrix area 5 (Table 1). The origin of this difference within QUE 99177 is not clear, but could be due to variable degrees of secondary processing in different parts of the meteorite or, possibly, to accretion from solar system reservoirs with distinct presolar grain abundances (Floss & Stadermann 2009a).

There has been much speculation in the literature about the relative scarcity of C isotopic anomalies compared to H and N anomalies, particularly given the fact that organic compounds appear to be the source of many of the D and ^{15}N enrichments (Sandford et al. 2001; Messenger et al. 2003; Floss et al. 2004). Although it does appear that chemical reactions that do not fractionate ^{12}C from ^{13}C play an important role in the formation of ^{15}N-rich carbonaceous matter that is not isotopically anomalous in C, as discussed above, the presence of abundant C-anomalous interstellar carbonaceous grains in the two CR3 chondrites studied here, indicates that secondary processes must also be important in accounting for the lack of such grains in most extraterrestrial materials.

Raman spectroscopy carried out on the IOM extracted from a variety of meteorites shows that CR chondrites contain the most primitive IOM of any meteorite group (Alexander et al. 2007; Busemann et al. 2007). Raman parameters such as G and D band widths are well-correlated with processes such as thermal metamorphism, terrestrial weathering, and amorphization due to space irradiation, and indicate that the IOM from CR chondrites has been largely unaffected by these processes (Busemann et al. 2007). Isotopic and elemental compositions indicate, further, that the IOM from the CR chondrites is similar to that found in IDPs and resembles the CHON particles from comet Halley (Alexander et al. 2007). The CR chondrites have experienced aqueous alteration that resulted in the formation of abundant phyllosilicates in these meteorites. However, aqueous alteration does not leave a characteristic Raman signature, and in general IOM appears to be relatively chemically inert during aqueous alteration (Busemann et al. 2007).

QUE 99177 and MET 00426 are the least altered members of the CR chondrite group, with low abundances of phyllosilicates or indeed any crystalline silicates compared to other members of this group (Abreu & Brearley 2006). Instead, the matrix material in these meteorites contains amorphous silicates resembling those seen in other primitive meteorites with high abundances of presolar grains, such as Acfer 094 and ALHA77307. Abreu & Brearley (2006) noted, moreover, the primitive nature of carbonaceous matter in QUE 99177 and MET 00426, emphasizing the low crystallinity of this material and the presence of detectable amounts of N indicative of low degrees of thermal metamorphism. The low degree of secondary processing undoubtedly accounts for the high abundances of O-anomalous and C-anomalous grains found in these meteorites by Floss & Stadermann (2009a) and in this study. As noted above, presolar SiC grains do not appear to be easily destroyed by aqueous alteration, as abundances are similar in CR1, CR2 (Davidson et al. 2009) and CR3 chondrites (this study). However, presolar silicate and oxide grains do seem to be affected by aqueous alteration: abundances are significantly higher in QUE 99177 and MET 00426 (Floss & Stadermann 2009a) than they are in CR2 chondrites such as Renazzo or NWA 530 (Nagashima et al. 2004; Floss & Stadermann 2005). Nagashima et al. (2005) also attributed the low abundance of presolar O-rich grains in the CM2 chondrite Murchison to the aqueous alteration experienced by this meteorite.

The discrepancy in the abundance of C-anomalous carbonaceous grains between the CR3 chondrites studied here and other primitive meteorites is probably also due to secondary processing. Alexander et al. (2007) have noted that the presence of

large bulk ^{15}N anomalies in the CR chondrites and their absence from other more heavily altered meteorites, such as the CI and CM chondrites and Tagish Lake, suggests that the carrier of these anomalies is quite fragile and is easily lost during mild low temperature aqueous alteration (Alexander et al. 2007). Indeed, Sephton et al. (2003) have carried out laboratory alteration experiments demonstrating that labile ^{15}N-enriched organic material is effectively removed during aqueous processing. Some loss of a heavy N component also appears to be due to thermal metamorphism of aromatic organic material (Busemann et al. 2007). Similarly, there is evidence for the loss of an isotopically light C component with increasing degree of thermal metamorphism (Busemann et al. 2007). NanoSIMS ion imaging work on matrix fragments from the Renazzo CR2 chondrite also provides evidence for loss of ^{15}N during such secondary processing (Floss & Stadermann 2005). Nitrogen isotopic compositions in Renazzo are ^{15}N-enriched, as expected in CR chondrites, but the magnitudes of the observed anomalies, with maximum δ^{15}N values up to 760‰ for hotspots and 190‰ for larger "bulk" regions, are significantly lower than those seen in QUE 99177 and MET 00426 (Floss & Stadermann 2009b) or in other primitive meteorites (Busemann et al. 2006a). Moreover, the only C-anomalous phases found in Renazzo matrix material are the two SiC grains noted earlier. No interstellar carbonaceous grains appear to be present, although one C-anomalous carbonaceous grain was found in the CR2 chondrite EET 92042 (Figure 5(b); Busemann et al. 2006b). This meteorite appears to have the most primitive and disordered IOM among the CR chondrites (Busemann et al. 2007; note that QUE 99177 and MET 00426 were not part of that study). Although the CR chondrites have largely escaped thermal metamorphism, there is disagreement about the maximum temperatures experienced by these meteorites during aqueous alteration (Krot et al. 2002). Estimates range from ∼100°C inferred from oxygen isotope studies (Clayton & Mayeda 1999) to ∼150°C based on phyllosilicate intergrowths and the absence of tochilinite (Zolensky 1991) and even up to ⩾250°C based on calcite compositions (Weisberg et al. 1994). Such temperatures, combined with aqueous alteration may suffice to destroy or isotopically exchange the relatively modest C isotopic anomalies observed in the interstellar carbonaceous grains that are still found in the less altered CR3 chondrites QUE 99177 and MET 00426.

4. CONCLUSIONS

QUE 99177 and MET 00426 are the first known CR3 chondrites and have largely escaped the aqueous alteration experienced by most of the CR chondrite group. In addition to high presolar silicate and oxide grain abundances (Floss & Stadermann 2009a), these meteorites also contain high abundances of phases with anomalous C isotopic compositions. Presolar SiC abundances are consistent with independent estimates for CR1 and CR2 chondrites (Davidson et al. (2009)), indicating that aqueous alteration does not destroy SiC, but are significantly higher than earlier abundance estimates based on noble gas contents (Huss et al. 2003). Most SiC grains are mainstream type, but two belong to type A+B and two are possible Y grains; this distribution is consistent with the relative abundances found in acid residue separations (Zinner 2004). Particularly notable are the high abundances of carbonaceous matter with anomalous C isotopic compositions. These grains probably formed in cold molecular clouds via UV photolysis of icy substrates; the observation of both ^{13}C-enriched and ^{13}C-depleted compositions suggests that multiple chemical pathways contribute to the formation of interstellar carbonaceous matter. Pathways that do not fractionate the C isotopes must also be important, as QUE 99177 and MET 00426 also contain numerous ^{15}N-rich hotspots of likely interstellar origin that do not contain C isotopic anomalies. C-anomalous material of interstellar origin has previously been found in IDPs and in IOM from primitive meteorites; however, the amounts observed in QUE 99177 and MET 00426 are significantly higher than in other primitive meteorites and attest to the primitive nature of these CR3 chondrites.

We would like to thank Tim Smolar for maintenance of the NanoSIMS and Auger Nanoprobe. Constructive and helpful comments by an anonymous reviewer are much appreciated. This work was funded by NASA grant NNX07AI45G (P.I.: C. Floss).

REFERENCES

Abreu, N., & Brearley, A. 2006, Lunar Planet. Sci., XXXVII, #2395
Abreu, N., & Brearley, A. 2008, Lunar Planet. Sci., XXXIX, #2013
Aléon, J., Engrand, C., Robert, F., & Chaussidon, M. 2001, Geochim. Cosmochim. Acta, 65, 4399
Aléon, J., Robert, F., Chaussidon, M., & Marty, B. 2003, Geochim. Cosmochim. Acta, 67, 3773
Alexander, C. M. O'D., Fogel, M., Yabuta, H., & Cody, G. D. 2007, Geochim. Cosmchim. Acta, 71, 4380
Alexander, C. M. O'D., Russell, S. S., Arden, J. W., Ash, R. D., Grady, M. M., & Pillinger, C. T. 1998, Meteorit. Planet. Sci., 33, 603
Amari, S., Anders, E., Virag, A., & Zinner, E. 1990, Nature, 345, 238
Amari, S., Lewis, R. S., & Anders, E. 1994, Geochim. Cosmochim. Acta, 58, 459
Amari, S., Nittler, L. R., Zinner, E., Gallino, R., Lugaro, M., & Lewis, R. S. 2001a, ApJ, 546, 248
Amari, S., Nittler, L. R., Zinner, E., Lodders, K., & Lewis, R. S. 2001b, ApJ, 559, 463
Bernatowicz, T., Fraundorf, G., Ming, T., Anders, E., Wopenka, B., Zinner, E., & Fraundorf, P. 1987, Nature, 330, 728
Bernatowicz, T., Messenger, S., Pravdivtseva, O. V., Swan, P., & Walker, R. M. 2003, Geochim. Cosmchim. Acta, 67, 4679
Bernstein, M. P., Elsila, J. E., Dworkin, J. P., Sandford, S. A., Allamandola, L. J., & Zare, R. N. 2002, ApJ, 376, 1115
Bernstein, M. P., Moore, M. H., Elsila, J. E., Sandford, S. A., Allamandola, L. J., & Zare, R. N. 2003, ApJ, 582, L25
Busemann, H., Alexander, C. M. O'D., & Nittler, L. R. 2007, Meteorit. Planet. Sci., 42, 1387
Busemann, H., Young, A. F., Alexander, C. M. O'D., Hoppe, P., Mukhopadhyay, S., & Nittler, L. R. 2006a, Science, 312, 727
Busemann, H., et al. 2006b, Lunar Planet. Sci., XXXVII, #2005
Busemann, H., et al. 2006c, Meteorit. Planet. Sci., 41, A34
Claus, G., & Nagy, B. 1961, Nature, 192, 594
Clayton, R. N., & Mayeda, T. K. 1999, Geochim. Cosmochim. Acta, 63, 2089
Childs, K. D., Carlson, B. A., LaVanier, L. A., Moulder, J. F., Paul, D. F., Stickle, W. F., & Watson, D. G. 1995, Handbook of Auger Electron Spectroscopy, (3rd ed., Eden Prairie, Minnesota: Physical Electronics)
Davidson, J., et al. 2009, Lunar Planet. Sci., XL, #1853
De Gregorio, B. T., Bassim, N. D., Cody, G. D., Nittler, L. R., Stroud, R. M., & Zega, T. J. 2008, Lunar Planet. Sci., XXXIX, #2139
Floss, C., & Stadermann, F. J. 2005, Lunar Planet. Sci., XXXVI, #1390
Floss, C., & Stadermann, F. J. 2008, Meteorit. Planet. Sci., 43, A44
Floss, C., & Stadermann, F. J. 2009a, Geochim. Cosmochim. Acta, 73, 2415
Floss, C., & Stadermann, F. J. 2009b, Lunar Planet. Sci., XL, #1083
Floss, C., Stadermann, F. J., Bradley, J. P., Dai, Z. R., Bajt, S., & Graham, G. 2004, Science, 303, 1355
Floss, C., Stadermann, F. J., Bradley, J. P., Dai, Z. R., Bajt, S., Graham, G., & Lea, A. S. 2006, Geochim. Cosmochim. Acta, 70, 2371
Garvie, L. A. J., Baumgardner, G., & Buseck, P. R. 2008, Meteorit. Planet. Sci., 43, 899
Gehrels, N. 1986, ApJ, 303, 336
Hoppe, P., Amari, S., Zinner, E., & Lewis, R. S. 1995, Geochim. Cosmochim. Acta, 59, 4029

Hoppe, P., & Ott, U. 1997, in Astrophysical Implications of the Laboratory Study of Presolar Materials, ed. T. Bernatowicz & E. Zinner (Woodbury, NY: AIP), 27
Huss, G., Meshik, A. P., Smith, J. B., & Hohenberg, C. 2003, Geochim. Cosmochim. Acta, 67, 4823
Jadhav, M., Amari, S., Zinner, E., & Maruoka, T. 2006, New Astron. Rev., 50, 591
Krot, A. N., Meibom, A., Weisberg, M. K., & Keil, K. 2002, Meteorit. Planet. Sci., 37, 1451
Langer, W. D., & Graedel, T. E. 1989, ApJSS, 69, 241
Langer, W. D., Graedel, T. E., Frerking, M. A., & Armentrout, P. B. 1984, ApJ, 277, 581
Lodders, K., & Amari, S. 2005, Chem. Erde, 65, 93
Martins, Z., et al. 2008, Meteorit. Planet. Sci., 43, A90
Messenger, S., Nakamura-Messenger, K., & Keller, L. P. 2008, Lunar Planet. Sci., XXXIX, #2391
Messenger, S., Stadermann, F. J., Floss, C., Nittler, L. R., & Mukhopadhyay, S. 2003, Space Sci. Rev., 106, 155
Messenger, S., & Walker, R. M. 1997, in Astrophysical Implications of the Laboratory Study of Presolar Materials, ed. T. J. Bernatowicz & E. Zinner (Woodbury, NY: AIP), 545
Mostefaoui, S., Zinner, E., Hoppe, P., Stadermann, F. J., & El Goresy, A. 2005, Meteorit. Planet. Sci, 40, 721
Nagashima, K., Krot, A. N., & Yurimoto, H. 2004, Nature, 428, 921
Nagashima, K., Sakamoto, N., & Yurimoto, H. 2005, Lunar Planet. Sci., XXXVI, #1671
Nakamura-Messenger, K., Messenger, S., Keller, L. P., Clemett, S. J., & Zolensky, M. E. 2006, Science, 314, 1439
Rodgers, S. D., & Charnley, S. B. 2008, MNRAS, 385, L48
Sandford, S. A., Bernstein, M. P., & Dworkin, J. P. 2001, Meteorit. Planet. Sci., 36, 1117
Sephton, M. A., Verchovsky, A. B., Bland, P. A., Gilmour, I., Grady, M. M., & Wright, I. P. 2003, Geochim. Cosmochim. Acta, 67, 2093
Stadermann, F. J., Floss, C., Bose, M., & Lea, A. S. 2009, Meteorit. Planet. Sci., in press
Terzieva, R., & Herbst, E. 2000, MNRAS, 317, 563
Tielens, A. G. G. M. 1997, in Astrophysical Implications of the Laboratory Study of Presolar Materials, ed. T. Bernatowicz & E. Zinner (Woodbury, NY: AIP), 523
Wasserburg, G. J., Boothroyd, A. I., & Sackmann, I. J. 1995, ApJ, 447, L37
Weisberg, M. K., Prinz, M., & Zolensky, M. E. 1994, Meteoritics, 29, 549
Zinner, E. 2004, in Meteorites, Planets and Comets,Vol. 1, ed. A. M. Davis (Amsterdam: Elsevier), 17
Zinner, E., Amari, S., Wopenka, B., & Lewis, R. S. 1995, Meteoritics, 30, 209
Zolensky, M. E. 1991, Meteoritics, 26, 414